Indian J. Phys. 82 (8) 987-1001 (2008)

IJP

Raman optical activity : a novel version of chiroptical spectroscopy

Moitrayee Mukherjee, Anamika Mukhopadhyay and Tapas Chakraborty*
Department of Physical Chemistry, Indian Association for the Cultivation of Science, Jadavpur, Kolkata-700 032, India

E-mail : pctc@iacs.res.in

Abstract : We present here an introductory review of Raman optical activity (ROA), a newly developed version of Raman spectroscopy suitable for predicting the absolute configuration of *chiral* molecules. The phenomenon involves minute differential scattering of the left and right circularly polarized lights from the *chiral* molecules, compared to the parent Raman scattering the ROA process is weaker by nearly three to five orders of magnitude. An operational theory of the phenomenon is presented with working equations. The connection between the experimentally observed quantities and the molecular parameters of interests is established. A brief description of the layout of the apparatus currently used for ROA measurements is presented along with a concise review of selected studies highlighting the possibilities of potential applications of this new version of chiroptical spectroscopy in the analysis of structural features of *chiral* molecules.

Keywords : Raman scattering, molecular vibrations, optical activity, circular dichroism, *chiral* molecules, absolute configurations

PACS No. : 33.20.Fb

1. Introduction

Polarization is an intrinsic attribute of Raman scattered light [1]. In early days of the discovery, the so called inelastically scattered Stokes shifted 'feeble fluorescence' noticed by Sir C V Raman and co-workers when dry and pure glycerine was irradiated by ultraviolet light appeared to be strongly polarized [2]. The universality of the feature, verified with more than sixty liquids at the time, was a clear indication to the investigators that the origin of the 'feeble fluorescence' was different from the ordinary fluorescence. The phenomenon, termed as Raman scattering, which appeared to be an optical analogue of Compton scattering, was interpreted in terms of transfer of a fraction of the light energy to the molecules leading to excitations of vibrational degrees of freedom of the latter. In recent years, using lasers of various temporal and spectral characteristics as excitation sources in combination with fast and ultrasensitive detection electronics, Raman spectroscopy has been turned into an indispensible tool for probing

*Corresponding Author

the structure and dynamical behaviour of large biomolecules in aqueous medium [1,3–6]. The polarization behaviour of the Raman scattered light, on the other hand, is exploited extensively in molecular spectroscopy in terms of depolarization ratio, an experimentally measured parameter, for symmetry designations of the vibrational normal modes.

A theory of the polarization behaviour of Raman scattered light from *chiral* molecules was presented by Atkins and Barron in the year 1969 [7]. It predicted that "the scattered light carries a very small degree of circular polarization and the scattered intensity is slightly different in right- and left-circular polarized incident light". This phenomenon is currently known as Raman optical activity (ROA). As Raman spectroscopy provides information about vibrational frequencies of a molecule, the significance of ROA is that it is basically a measure of vibrational optical activity (VOA). A simultaneous measurement of normal Raman and ROA spectra should provide richer information about the configuration of a *chiral* molecule. In this regard, ROA is expected to be more informative compared to the standard electronic circular dichroism (ECD) spectroscopy performed routinely for configurational analysis of biomolecules in the electronic absorption region [8]. An electronic CD spectrum provides configurational information of a *chiral* molecule around its UV absorbing chromophore. If the molecule lacks such a chromophore, it is inaccessible to CD. On the other hand, the ROA transitions are associated with Raman active vibrational transitions, which usually are normal modes and comprised of atoms involving the entire skeleton of the *chiral* molecule. Thus, presence of any special type of chromophore in the molecule is not required. The sign and magnitude of each band in a ROA spectrum contains information about the absolute configuration of the molecule.

Another version of vibrational optical activity, which corresponds to measurements of differential absorption cross-sections of vibrational transitions by left and right circularly polarized infrared light, is known as vibrational circular dichroism (VCD) [8,9]. From vibrational spectroscopic viewpoints, as normal Raman and infrared absorption are complementary to each other [1], the ROA and VCD are also expected to be complementary techniques. However, the physical origins of the two processes are different [8]. While VCD corresponds to interaction between vibrationally induced changes in electric dipole moment of the molecule with its magnetic counterpart, the ROA depends on interaction of changes in electric polarizability with the respective magnetic dipole and electric quadrupole moments induced by molecular vibrations. Because of these differences, the two techniques are used to probe different aspects of molecular *chirality*. For example, the VCD bands for the characteristic amide vibrational transitions in peptides and proteins differ in frequency, intensity and sign pattern in various secondary structures. On the other hand, the sign pattern of the ROA bands of peptides are found to be somewhat insensitive to changes in secondary structures, and only the frequencies of the bands show usual shifts with small changes

in intensities. VCD is sensitive to the changes in overall molecular *chirality*, but ROA is more sensitive to the backbone structure, and in this sense, the two techniques are truly complementary to each other.

However, the main limitation of ROA is that it is an extremely weak effect, and compared to normal Raman process, which itself is a very weak scattering phenomenon having a cross-section of 10^{-30} to 10^{-25} cm^2/molecule, the former is three to five orders of magnitude weaker. Thus, identification of true ROA signals from the experimental artefacts is a tricky matter in measurements, and the first reliable ROA spectra of the two enantiomets of 1-phenylethanol and 1-phenylethylamine were reported only in the year 1973 [10]. Furthermore, the detailed features of a ROA spectrum are quite sensitive to the optical arrangement of the measurement, *i.e.*, directions of signal collection with respect to propagation direction of the incident laser light to the sample (shown below). Because of such intricacies of measurements, its practice was limited, until very recently, within a handful of experimental groups. However, with the realization of its potential applications in biology, a commercial equipment has been introduced (*Chiral* RAMAN, Bio Tools Inc.), and ROA spectral measurement of *chiral* molecules is now a routine affair. However, correct interpretation of ROA spectra, and assignments of absolute configurations of *chiral* molecules on the basis of the measured data, are heavily dependent on accurate quantum mechanical predictions of the spectra and other molecular parameters [8].

For enhancements of ROA signals from *chiral* molecules in dilute solutions, two extensions of the effect were theoretically proposed and experiments corresponding to those suggestions have also been demonstrated in recent years [11]. One of the suggested enhancement mechanisms is to combine the ROA effect with Plasmon resonances generated by certain metal surfaces [12], and the phenomenon is called surface enhanced Raman optical activity (SEROA). Surface enhancement of Raman signals over conventional Raman scattering intensities is widely used in various branches of Science and Technology, and typical enhancement occurs by a factor of ~10^3–10^6 [11]. However, the general appearance of SEROA spectra are somewhat different from the corresponding ROA spectra indicating that in addition to surface enhancement, the spectra are modified due to interaction of the molecules with surfaces. The second enhancement mechanism is by selecting the laser wavelength close to an electronic absorption band of the molecule, *i.e.*, resonance enhancement, and the effect is called resonance Raman optical activity (RROA) [13]. In a resonance Raman process, the enhancement factor is typically several orders of magnitude compared to the normal process. The theory of RROA has been extended to the case of strong resonance with a single electronic state, and it predicts that the intensities of RROA bands are proportional to those in a parent resonance Raman (RR) spectrum. Experimental demonstration of RROA measurement was reported nearly a decade ago, the observations were mostly consistent with the predictions of theory.

In the following sections, we introduce a working theory of the ROA process discuss two different versions of the apparatus currently used in several laboratories and review a few selected studies to give a feel of development in this important direction of Raman Spectroscopy.

2. Operational theory of ROA

The basic theory of ROA was first given by Atkins and Barron [7]. The phenomenon was shown as the effect of interference between the waves scattered *via* the polarizability and electric dipole-magnetic dipole optical activity tensor. Subsequently, a more sophisticated theory was proposed by Barron and Buckingham taking into account of the electric dipole-electric quadrupole optical activity tensor in addition to the former [14]. In this theory, the electric vectors of the radiation emitted by the induced oscillating electric dipole, magnetic dipole and electric quadrupole of the molecule due to interaction with the incident left and right circularly polarized lights were considered, and the associated intensities (which are proportional to the square of the electric field vectors) were calculated. The real oscillating electric dipole, magnetic dipole and quadrupole moments induced in the molecule by the real part of the electric and magnetic vectors of the light and electric field gradient $\nabla_\alpha E_\beta$ (calculated at the molecular origin) of the incident radiation, at far from resonance condition, are given by the following equations [15] :

$$\mu_\alpha = \alpha_{\alpha\beta} E_\beta + \frac{1}{\omega} G'_{\alpha\beta} \dot{B}_\alpha + \frac{1}{3} A_{\alpha\beta\gamma} \nabla_\beta E_\gamma + \cdots, \tag{1}$$

$$m_\alpha = -\frac{1}{\omega} G'_{\alpha\beta} \dot{E}_\beta + \cdots, \tag{2}$$

$$\Theta_{\alpha\beta} = A_{\alpha\beta\gamma} E_\gamma + \cdots, \tag{3}$$

where,

$$\alpha_{\alpha\beta} = \frac{2}{\hbar} \sum_{j \neq n} \frac{\omega_{jn}}{\omega_{jn}^2 - \omega^2} \mathrm{Re} \left\{ \langle n | \mu_\alpha | j \rangle \langle j | \mu_\beta | n \rangle \right\}, \tag{4}$$

$$G'_{\alpha\beta} = -\frac{2}{\hbar} \sum_{j \neq n} \frac{\omega}{\omega_{jn}^2 - \omega^2} \mathrm{Im} \left\{ \langle n | \mu_\alpha | j \rangle \langle j | m_\beta | n \rangle \right\}, \tag{5}$$

$$A_{\alpha\beta\gamma} = \frac{2}{\hbar} \sum_{j \neq n} \frac{\omega_{jn}}{\omega_{jn}^2 - \omega^2} \mathrm{Re} \left\{ \langle n | \mu_\alpha | j \rangle \langle j | \Theta_{\beta\gamma} | n \rangle \right\}, \tag{6}$$

n = Initial state, j = virtual intermediate state of the molecule,

$\alpha_{\alpha\beta}$ = Polarizability tensor responsible for conventional Raman scattering,

$G'_{\alpha\beta}$ = Electric dipole-magnetic dipole optical activity tensor whose isotropic component

is responsible for optical rotation in fluid,

$A_{\alpha\beta\gamma}$ = Electric dipole-electric quadrupole optical activity tensor responsible for additional contribution to optical rotation of oriented samples.

The details of the theory can be found in the original publication of Barron and Buckingham [15]. We consider here only the terms essential to define the ROA observables.

The intensity difference of the scattered left and right circularly polarized light, $(I_R - I_L)$, is the ROA observable quantity. Barron and Buckingham introduced the term $\Delta = (I_R - I_L)/(I_R + I_L)$, and called it the circular intensity difference (CID).

The spontaneous ROA can be measured by the following two experimental schemes (Figure 1).

(1) Incident circular polarization (ICP) : The incident lights are left and right circularly polarized and the scattered light of any polarization can be detected (Figure 1A).

(2) Scattered circular polarization (SCP) : The incident light is linearly polarized or depolarized and the left and right circular polarization components of the scattered light are detected (Figure 1B).

In an ICP experiment, the intensity of the scattered light can be measured parallel (0°), anti-parallel (180°), or perpendicular (90°) to the direction of incident light. In right angle scattering, the polarized and depolarized scattered rays can be measured. In the former case, the analyzer axis is perpendicular (x) and in latter parallel (z) to the scattering plane (yz).

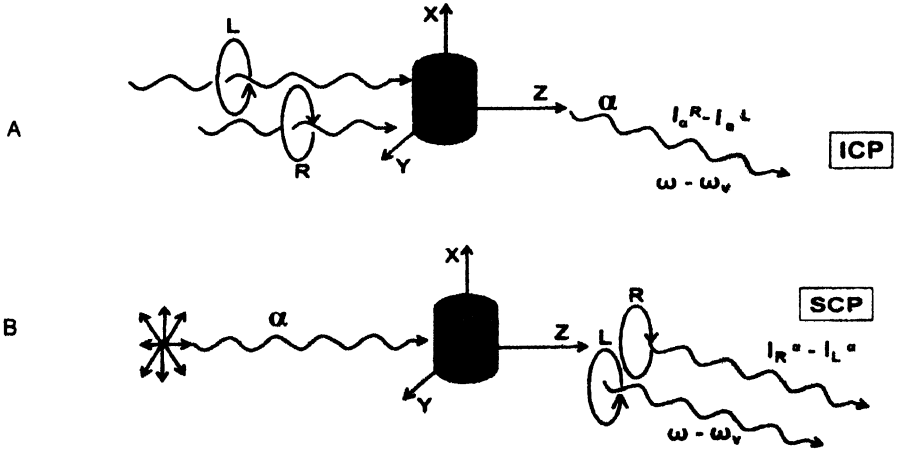

Figure 1. Schematic representation of ICP and SCP modes of ROA process. Here, α = linear polarization parallel or perpendicular to the plane of observation or depolarization for incident radiation, L = left polarization, R = right polarization, ω = frequency of incident radiation, $\omega - \omega_v$ = Stokes shifted vibrational Raman scattered frequency.

The expressions for the CIDs in the three mentioned directions in an ICP experiment, calculated by a semi-classical treatment, [15] are as follows

$$\Delta(0^\circ) = \frac{8\left[45\alpha G' + \beta(G')^2 - \beta(A)^2\right]}{2c\left[45\alpha^2 + 7\beta(\alpha)^2\right]}, \tag{7}$$

$$\Delta(180^\circ) = \frac{48\left[\beta(G')^2 + 1/3\beta(A)^2\right]}{2c\left[45\alpha^2 + 7\beta(\alpha)^2\right]}, \tag{8}$$

$$\Delta_x(90^\circ) = \frac{2\left[45\alpha G' + 7\beta(G')^2 + \beta(A)^2\right]}{c\left[45\alpha^2 + 7\beta(\alpha)^2\right]}, \tag{9}$$

$$\Delta_z(90^\circ) = \frac{12\left[\beta(G')^2 - 1/3\beta(A)^2\right]}{6c\beta(\alpha)^2}. \tag{10}$$

The isotropic invariants of the polarizability tensor and the electric dipole-magnetic dipole optical activity tensor are defined as

$$\alpha = \frac{1}{3}\alpha_{\alpha\alpha} = \frac{1}{3}\left(\alpha_{xx} + \alpha_{yy} + \alpha_{zz}\right), \tag{11}$$

$$G' = \frac{1}{3}G'_{\alpha\alpha} = \frac{1}{3}\left(G'_{xx} + G'_{yy} + G'_{zz}\right), \tag{12}$$

and the anisotropic invariants of the polarizability-polarizability and polarizability-optical activity tensor component products are defined as

$$\beta(\alpha)^2 = \frac{1}{2}\left(3\alpha_{\alpha\beta}\alpha_{\alpha\beta} - \alpha_{\beta\beta}\right), \tag{13}$$

$$\beta(G')^2 = \frac{1}{2}\left(3\alpha_{\alpha\beta}G'_{\alpha\beta} - \alpha_{\alpha\alpha}G'_{\beta\beta}\right), \tag{14}$$

$$\beta(A)^2 = \frac{1}{2}\omega\alpha_{\alpha\beta}\varepsilon_{\alpha\gamma\delta}A_{\gamma\delta\beta}. \tag{15}$$

Considering the bond polarizability model which assumes that the polarizability and optical activity tensors of the whole molecule can be taken as sum of the contributions of local groups present in the molecule, and considering the groups to be cylindrically symmetric, the above equations are modified as : $\alpha G' = 0$ *i.e.*, isotropic ROA vanishes, and $\beta(G')^2 = \beta(A)^2$, *i.e.*, magnetic dipole and electric quadrupole anisotropic contributions become equal. The corresponding CIDs for backward and forward directions are

$$\Delta(0^\circ) = 0, \tag{16},$$

$$\Delta(180°) = \frac{32\beta(G')^2}{c\left[45\alpha^2 + 7\beta(\alpha)^2\right]} \quad . \tag{17}$$

From equations 16 and 17 it is evident that the backward scattering is the most favorable direction for ROA measurement among the four directions represented by equations 7–10.

Another suggested experimental configuration is to measure the right angle scattered intensity by setting the analyzer axis at *magic angle,* 54.74°, to the scattering plane (*yz*). In this orientation the contribution of electric dipole-electric quadrupole optical activity tensor vanishes. The corresponding expression for CID is the following :

$$\Delta^*(90°) = \frac{20/3\left[9\alpha G' + 2\beta(G')^2\right]}{10/3c\left[9\alpha^2 + 2\beta(\alpha)^2\right]} \quad . \tag{18}$$

3. Experimental layout

As stated in the previous section, the scattered ROA intensity sensitively depends on the direction of signal collection with respect to the propagation direction of the incident laser beam and scattering plane [15]. Below, we describe the schematics of two experimental schemes (ICP and SCP) considering backscattering signal collection geometry which is preferred over the polarized right-angle scattering geometry configuration commonly used in emission spectroscopy.

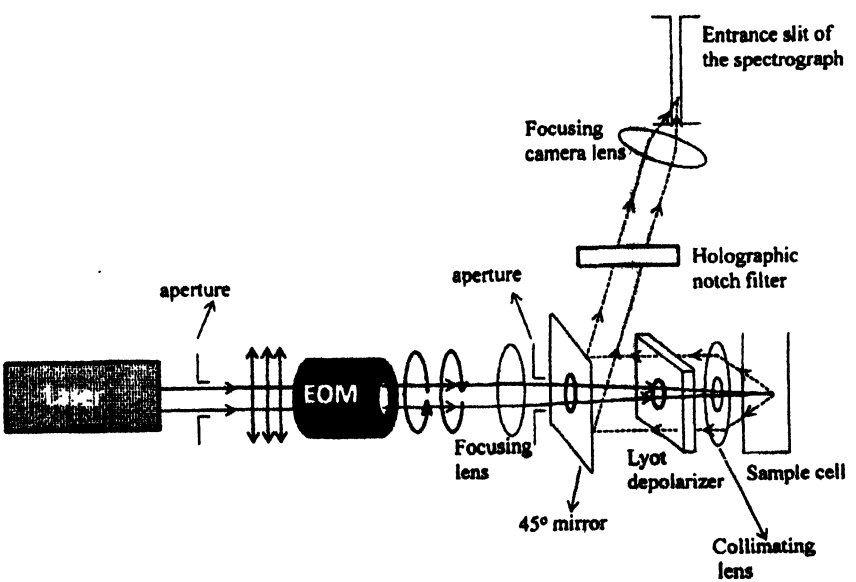

Figure 2. Experimental scheme of ICP ROA measurements in backscattering geometry.

In Figure 2 we have presented a schematic diagram of the ROA apparatus based on the one developed by the group of Laurence D Barron at the University of Glassgow [16,17]. The excitation light source is the 514.5 nm line of an argon-ion laser. In Raman spectroscopic measurements, this excitation wavelength is mostly preferred because it is a compromise between two opposing effects of lowering of scattered intensity as the excitation wavelength moves towards red, and interference arising from background fluorescence signal for electronic excitations of different chromophores in samples on shifting the excitation wavelengths to blue. A *backthinned* cooled CCD is typically used as detector as in normal Raman spectroscopy. Such detectors have extremely low noise level, and the quantum efficiency is 80% in the spectral range of 450–600 nm. The optical system is a usual 'mirror with a hole' arrangement, typically used in backscattering Raman measurements. A calcite Lyot depolarizer with a small central hole is used to depolarize the backscattered cone of Raman light, and a lens with a small central hole to collimate the backscattered depolarized Raman light before it strikes the 90° deflecting mirror.

The principle of measurement is the following. First, the linearly polarized laser light is allowed to pass through an electro-optic modulator (EOM) to convert the linearly polarized light to 'right' or 'left' circularly polarized light by applying quarter wave voltages across the EOM electrodes. The EOM has a longitudinal Pockel cell based on KDP crystal which is kept under thermal stabilization to eliminate birefringence drift caused by external temperature fluctuations. To match the longitudinal axis of the EOM crystal along the laser beam it is placed on high-precision movable stage. The generated circularly polarized light is focused by a planoconvex synthetic fused-silica lens into a standard glass cell containing typically 200–300 μl of a liquid sample. The cell is mounted also on a XYZ translational stage. In between the focusing lens and sample, a centrally holed Lyot depolarizer is placed. The depolarizer consists of two calcite crystal plates and collects the backscattered light emerging from the sample. The optical axes of these two crystals kept at 45 ± 0.2° with respect to each other. The collimated depolarized light is deflected at right angle by a plane eliptical mirror. The Lyot depolarizer, collimating lens and the mirror are also placed on a XYZ translational stage. The deflected scattered light reaches a spectrograph after passing through a notch filter for elimination of Rayleigh scattered light and focused by a camera lens. The spectral resolution of the spectrographs used is typically 5 cm^{-1}. A PC is used for data collection. The circular intensity difference (CID), $(I^R - I^L)/(I^R + I^L)$, is generated and recorded as a function of wavelength of the scattered light.

Although the design of the ICP ROA instrument described above appears to be quite straight forward, but it has several demerits. During measurements, 'flicker noise' arising from dust particles, density fluctuations, laser power fluctuations, *etc.* result in lowering of the signal to noise ratio (SNR). Secondly, the right or left circularly polarized output lights of EOM do not pass through the sample at the same time.

Therefore, fluctuations of two polarization components are not synchronized. These drawbacks are mostly eliminated in SCP strategy of detection. This is because, the two circularly polarized components in the scattered light are seperated at the same time resulting in cancellation of flicker noise and gives much superior signal-to-noise characteristics of the recorded spectra.

The basic design of SCP for backscattering geometry (Figure 3) is the following [18]. Linearly polarized 532 nm laser light emerging from a frequency-doubled Nd : YAG laser passes through a polarization 'scrambler' which scrambles the initial polarization of the incident laser light by a fast rotation of the azimuth. The depolarized light reaches sample cell following deflection from a tiny prism. The backscattered collected light containing both right and left circularly polarized components is converted into linear polarization states with azimuth perpendicular and parallel, respectively with

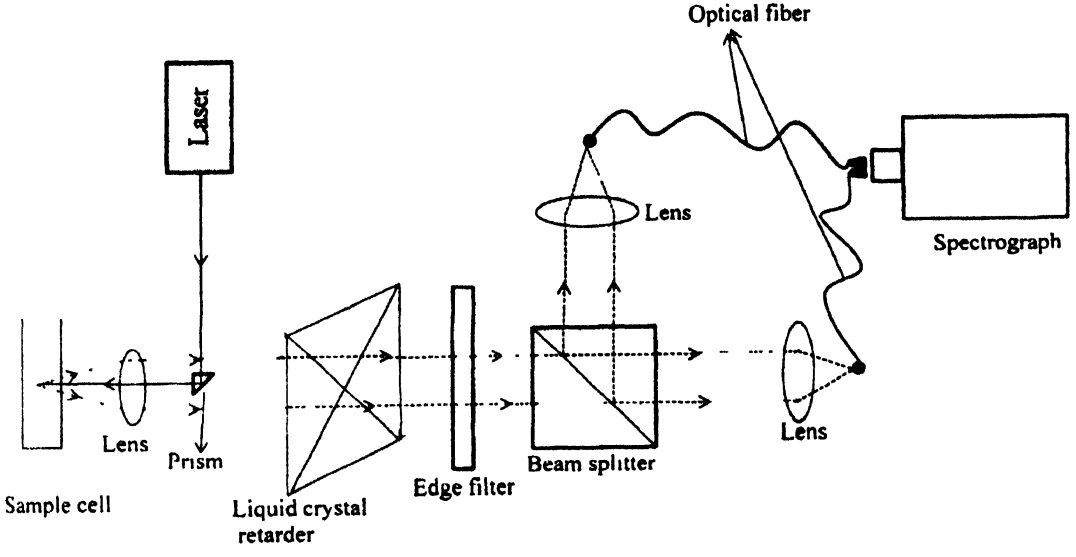

Figure 3. Experimental scheme of SCP ROA measurement in backscattering geometry

respect to the plane of the instrument by passing the scattered light through a liquid crystal retarder. A notch filter is used to eliminate the Rayleigh scattered light. At the beam-splitter, the perpendicular polarization component is reflected at 90° to the propagation direction and the parallel polarization component remains undiverted. These two differently polarized scattered light components are sent to an imaging spectrograph *via* two optical fibers and detected on two segments of the same chip, one above other. The difference between the signals of the two segments for each wavelength gives the required ROA spectrum.

4. Selected examples of ROA studies

In the past two decades, ROA spectra of a wide variety of *chiral* molecules have been

investigated, starting from small organic molecules, amino acids, peptides, proteins up to intact viruses. Advancement of instrumentations in the recent years has played a major role in making ROA studies on complex systems possible. However, like in all branches of spectroscopy, real potential of a method is best evaluated by scrutinizing in what details information of a small molecule can be obtained. In the following paragraphs we cite a few representative ROA studies from literature. For better appreciation of the merits of the technique, we shall limit our discussion to the domain of smaller molecules. A number of excellent reviews and original articles are available in the literature where the reader can find reports of ROA studies on large biomolecules [19,20].

We begin illustrating the normal Raman and ROA spectra (Figure 4) of pure *R* and *S* enantiomers of α-pinene, a naturally occurring bicyclic *chiral* hydrocarbon

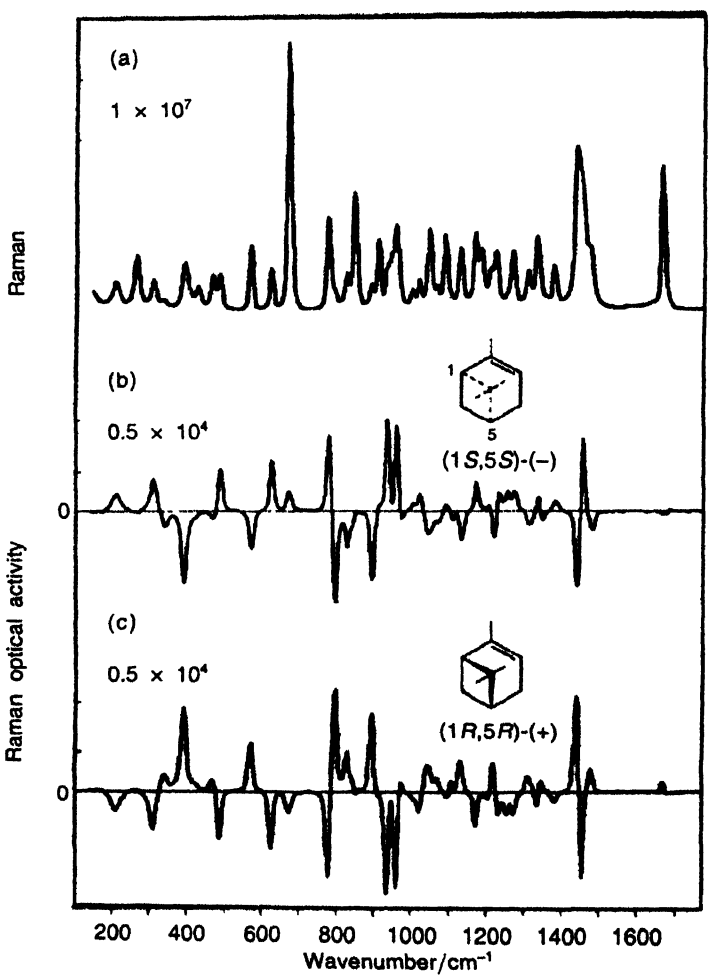

Figure 4. (a) Raman spectrum of the two enantiomers of α-pinene and (b, c) Raman spectra of the two isomers of the molecule (taken from Ref. [19]).

compound containing two *chiral* centres at 1 and 5 positions, reported recently by Barron *et al* [19]. All three spectra presented here were measured in backscattering geometry. The vibrational bands displayed in the Raman spectra of both the enantiomers are same (Figure 4a) and those correspond mostly to the fundamentals of ring deformation, C–C stretching and C–H bending modes. The broad feature near 1450 cm^{-1} is due to the fundamental of C=C stretching. A comparison between the three spectra shows that nearly all Raman bands are optically active, and the ROA spectra of the two enantiomers (Figure 4b-c) are perfect mirror-symmetric to each other. The C=C stretching band and a few others display strong couplet type transitions in the ROA spectra. It is obvious that every bit of the ROA spectrum of an enantiomer has bearing of its absolute configuration. The unknown configuration of the enantiomerically pure sample of a compound is obtained by correlating the measured ROA spectrum with the theoretically predicted spectra of all possible conformations of the molecule, which are obtained performing density functional theory or *ab initio* calculations at decent levels of theory.

As second example, we cite a study which demonstrates that the detailed features of a ROA spectrum dependent on the mode of signal collection with respect to propagation direction of the incident laser beam. It has been mentioned in the previous section that to come to the final expressions of CID for various scattering geometries, a number of assumptions were considered. The spectral appearance of

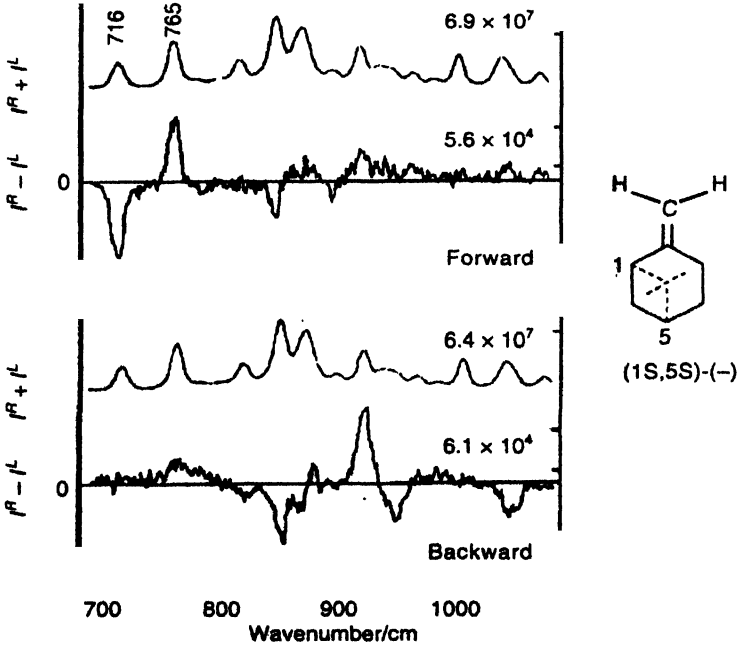

Figure 5. A comparison of normal Raman and ICP ROA spectra of (1*S*,5*S*)-(–) β-pinene for two different signal collection geometries (taken from Ref. [20]).

the absolute configurations of a *chiral* molecule. An interesting illustration in this regard was reported recently by Hug and co-workers in the journal *Nature* concerning assignment of the absolute configuration of partially deuterated *chiral* Neopentane (CHD_2-$C(CH_3)(CD_3)$-CH_2D) [22]. Here, *chirality* arises because of dissymmetric mass distribution by the isotopic substitutions. Because of chemical inertness of the compound and for lacking of any specific chromophore, conventional methods for assigning absolute configurations, like diastereomeric interactions with other *chiral* molecules, or optical rotation and ECD are not applicable. On the other hand, ROA being a vibrational optical activity method, it is applicable in difficult situations, as in the present case. In Figure 7 we reproduce from Ref. 22 the ROA spectra of an *enantiomeric* form of the molecule (pure sample) recorded at two different temperatures (0 and 25 °C) in the frequency range of 720–1350 cm^{-1} (top two traces). Large modulations in signs of the bands occur in the frequency span of 720–950 cm^{-1}, and this region is dominated by modes involving the rocking motions of the whole methyl groups. In 1150–1350 cm^{-1} range, C–C stretching and deformations of the methyl groups are important. The molecule exists over nine different rotameric forms, and calculation shows that the signs of the ROA bands are significantly different from one rotamer to other (bottom trace). A superposition of the calculated spectra of the nine rotamers for the *R* enantiomeric form of the molecule is shown in *part c* of the figure. Comparison of the top three traces clearly shows that the match between the experimental and computed spectra for the mixture is excellent, although the spectra of the individual rotamers, in terms of the signs of the bands, are very different from the measured ones. Thus, the sample probed by ROA measurement could be assigned to *R* enantiomeric form of the molecule with confidence. However, it is obvious that the success of the ROA method in configurational analysis is immensely dependent on accurate spectral predictions by theoretical methods. In fact, it is an area where synergy between theory and experiment can play an important role.

5. Concluding Remarks and Outlook

We reiterate that the review on Raman Optical Activity presented here is by no means a comprehensive one. Our purpose is to introduce the subject to the readers interested in Raman spectroscopy and its recent advancements in molecular structure analysis, particularly for studies in the liquid phase. A few select studies cited here, following a brief introduction to operational part of the theory of ROA and instrumentation, show the rich information content of a ROA spectrum pertaining to handedness of a *chiral* molecule, the technical intricacies of ROA measurements and potentials of ROA in biomolecular structure analysis in water medium. Since Raman scattering is intrinsically an ultrafast process and a Raman spectrum gives a snapshot of vibrational modes of the molecule under study, ROA could be used as an immensely useful technique to monitor the progress of chemical events involving *chiral* reactant and product molecules,

and dynamical studies concerning conformational evolution of complex *chiral* molecules under external stimulus, like sudden change in temperature, exposure to light, *etc.* However, as stated before, the success of the method is enormously dependent on accurate theoretical predictions of ROA spectra of molecules by quantum chemical methods. In recent years, tremendous progress has been made in development of powerful algorithms for calculation of ROA spectra of relatively large molecules with reasonable accuracy. With availability of commercial equipment and powerful software packages for predicting spectra, more ROA studies addressing interesting problems concerning wider issues of structure and dynamics of complex *chiral* systems are expected in the years to come. Raman effect was discovered eighty years ago, but much of its potential is yet to be explored.

References

[1] J J Laserna *Modern Techniques in Raman Spectroscopy* (John Wiley & Sons) (1996)

[2] C V Raman *Indian J. Phys.* **2** 387 (1928)

[3] W W Parson *Modern Optical Spectroscopy* (Berlin . Springer-Vergal) (2007)

[4] Z Q Tian *J. Raman Spectrosc.* **36** 466 (2005)

[5] D Pestov, M Zhi, Z E Sariyanni, N G Kalugin, A A Kolomenskii, R Murawski, G G Paulus, V A Sautenkov, H Schuessler, A V Sokolov, G R Welch, Y V Rostovtsev, T Siebert, D A Akimov, S Graefe, W Kiefer and M O Scully *Proc Natl Acad Sci.* **102** 14976 (2005)

[6] D Pestov, X Wang, G O Ariunbold, R K Murawski, V A Sautenkov, A Dogariu, A V Sokolov and M O Scully *Proc Natl. Acad. Sci* **105** 422 (2008)

[7] P W Atkins and L D Barron *Mole. Phys* **16** 453 (1969)

[8] N Berova, K Nakanishi and R W Woody *Circular Dichroism : Principles and Applications* (2nd Edn) (Wiley-VCH) (2000)

[9] P L Polavarapu *Chirality* **20** 664 (2008)

[10] L D Barron, M P Bogaard and A D Buckingham *J. Am. Chem Soc* **95** 603 (1973)

[11] S Abdali and E W Blanch *Chem Soc Rev* **37** 980 (2008)

[12] S Efrima *J. Chem Phys.* **83** 1356 (1985)

[13] M Vargek, T B Freedman, E Lee and L A Nafie *Chem. Phys. Lett.* **287** 359 (1998)

[14] L D Barron and A D Buckingham *Mole. Phys.* **20** 1111 (1971)

[15] L D Barron *Molecular Light Scattering and Optical Activity* (2nd Edn) (Cambridge · Cambridge University Press) (2004)

[16] J Hanzlíková, P Praus and V Baumruk *J. Mol. Struct* **480** 431 (1999)

[17] L Hecht and L D Barron *Faraday Discuss.* **99** 35 (1994)

[18] W Hug *J. Raman Spectrosc.* **30** 841 (1999)

[19] L D Barron, L Hecht, I H McColl and E W Blanch *Mol. Phys.* **102** 731 (2004)

[20] L D Barron, F Zhu and L Hecht *Vib. Spect.* **42** 15 (2006)

[21] C N Tam, P Bour and T A Keiderling *J. Am. Chem. Soc.* **119** 7061 (1997)

[22] J Haesler, I Schindelholz, E Riguet, C G Bochet and W Hug *Nature* **446** 526 (2007)